NASA Technical Memorandum 78490

(NASA-TM-78490) SOLUTION OF TRANSONIC FLOWS BY AN INTEGRO-DIFFERENTIAL EQUATION METHOD (NASA) 30 p HC A03/MF A01 CSCL 20D

N78-26391

Unclas

G3/34 23343

Solution of Transonic Flows by an Integro-Differential Equation Method

Wandera Ogana

June 1978

National Aeronautics and
Space Administration

NASA Technical Memorandum 78490

Solution of Transonic Flows by an Integro-Differential Equation Method

Wandera Ogana, Ames Research Center, Moffett Field, California

NASA

National Aeronautics and
Space Administration

Ames Research Center
Moffett Field, California 94035

NOMENCLATURE

$F(\bar{x})$	thickness distribution
$H(\bar{x})$	distribution of camber
h_i	half of the height of Δ_i; $2h_i = r_i + q_i$
K	transonic similarity parameter, $K = \dfrac{1 - M_\infty^2}{M_\infty^{4/3}\delta^{2/3}}$
M	number of intervals into which the airfoil is divided by rectangular elements
M_∞	free-stream Mach number
n	number of rectangular elements or mesh points
P	$\equiv (x,y)$
P_i	$\equiv (x_i,y_i)$
Q	$\equiv (\xi,\zeta)$
q_i	magnitude of the difference between y_i and the y-coordinate of the bottom edge of Δ_i
r_i	magnitude of the difference between y_i and the y-coordinate of the top edge of Δ_i
$\bar{u}$, $\bar{v}$	velocity components in the tangential and transverse directions, respectively, $\bar{u} = \dfrac{\partial\bar{\phi}}{\partial\bar{x}}$, $\bar{v} = \dfrac{\partial\bar{\phi}}{\partial\bar{y}}$
u, v	velocity components in the transformed plane, $u = \dfrac{\partial\phi}{\partial x}$, $v = \dfrac{\partial\phi}{\partial y}$
u_i	tangential velocity at the ith mesh point
$\bar{x},\bar{y}$	rectangular Cartesian coordinates in the physical plane
x,y	rectangular Cartesian coordinates in the transformed plane, $x = \bar{x}$, $y = \beta\bar{y}$
x_i,y_i	coordinates of the ith mesh point
$\bar{Y}_+(\bar{x})$, $\bar{Y}_-(\bar{x})$	upper and lower airfoil profiles, respectively
$Y_\pm(x)$	modified airfoil profile, $Y_\pm(x) = \left[\dfrac{\gamma + 1}{\delta K^{3/2}}\right]\bar{Y}_\pm(\bar{x})$

α	angle of attack, deg
β	Prandtl-Glauert parameter, $\beta = \sqrt{1 - M_\infty^2}$
γ	ratio of specific heats
$\gamma(x)$	vortex strength, $\gamma(x) = u(x,+0) - u(x,-0)$
γ_i	$= \gamma(x_i)$
$\Delta u^2(x,y)$	$= u^2(x,y) - u^2(x,-y)$
$\Delta\phi_\zeta(\xi)$	$= \dfrac{dY_+}{d\xi} - \dfrac{dY_-}{d\xi}$
Λ_i	the ith rectangular element
δ	thickness ratio
δ_i	half the width of Λ_i
ε	half the width of σ_ε
λ	aspect ratio of σ_ε
μ	$= \dfrac{2(\gamma + 1)}{\delta K^{3/2}}$
ξ, ζ	rectangular Cartesian coordinates
σ_ε	the vanishing rectangular cavity
τ	measure of the distribution of camber
$\bar{\phi}(\bar{x},\bar{y})$	perturbation velocity potential
$\phi(x,y)$	modified perturbation velocity potential, $\phi(x,y) = \left[\dfrac{(\gamma + 1)M_\infty^2}{\beta^2}\right]\bar{\phi}(\bar{x},\bar{y})$
$\phi_L(x,y)$	contribution to potential due to lifting effects
ϕ_{L_i}	$= \phi_L(x_i,y_i)$
$\phi_N(x,y)$	contribution to potential due to nonlifting effects
ϕ_{N_i}	$= \phi_N(x_i,y_i)$

SOLUTION OF TRANSONIC FLOWS BY AN

INTEGRO-DIFFERENTIAL EQUATION METHOD

Wandera Ogana*

Ames Research Center

SUMMARY

For free-stream Mach numbers less than unity, steady transonic flow past a two-dimensional airfoil is described by a singular integro-differential equation which involves the tangential derivative of the perturbation velocity potential. The integro-differential equation can be transformed into a nonlinear system of algebraic equations involving numerical evaluation of a first-order derivative. Subcritical flows are solved by a central difference approximation of the derivative everywhere. For supercritical flows with shocks, central differences are taken in locally subsonic flow regions and backward differences in locally supersonic flow regions. A normal shock condition is applied. A condition is enforced at the sonic point which ensures smooth transition from subsonic to supersonic velocities. The region of integration is partitioned into rectangular elements whose sizes can be adjusted in order to minimize the number of mesh points. The method is applied to a nonlifting parabolic-arc airfoil in both subcritical and supercritical flows, and to a subcritical flow over a lifting NACA 0012 airfoil. Although a small number of mesh points is used, the results compare favorably with finite difference results. For lifting flows, a modified boundary condition should be applied to improve the accuracy of the results at the leading edge of the airfoil.

INTRODUCTION

The transonic small perturbation equation for steady, two-dimensional flows is transformable to a singular integro-differential equation which can be differentiated to yield a singular integral equation in the tangential velocity (refs. 1 and 2). Solutions of the integral equation have been obtained for subcritical flows (refs. 3-6) and for embedded supersonic regions with shock waves (refs. 3, 4 and 7). The transonic integro-differential equation has not been solved numerically. A related linear integral equation for three-dimensional subsonic flows has been studied by Morino and Kuo (ref. 8). The present method solves the integro-differential equation using a technique which Ogana (refs. 6 and 9) developed for the transonic integral equation. Solutions for supercritical flows with shocks can be determined by taking

---

*NRC Research Associate (1976-1977). Presently a Lecturer at University of Nairobi, Department of Mathematics, P.O. Box 30197, Nairobi, Kenya.

central differences in local subsonic flow regions and backward differences in local supersonic flow regions as proposed by Murman and Cole (ref. 10). Special consideration is given to sonic and shock points. An advantage of the integro-differential equation method over the integral equation method is that the shock conditions can be introduced in a simple direct manner.

INTEGRO-DIFFERENTIAL EQUATION

We consider steady, two-dimensional transonic flow past a thin airfoil of thickness ratio δ, and measure of the amount of camber τ, at a small angle of attack α. For subsequent convenience of notation, the rectangular Cartesian coordinates in the physical plane are taken to be $(\bar{x},\bar{y})$. Let the upper airfoil profile be described by

$$\bar{Y}_{+}(\bar{x}) = \delta F(\bar{x}) + \tau H(\bar{x}) - \alpha\bar{x} \tag{1a}$$

and the lower profile by

$$\bar{Y}_{-}(\bar{x}) = -\delta F(\bar{x}) + \tau H(\bar{x}) - \alpha\bar{x} \tag{1b}$$

where $F(\bar{x})$ and $H(\bar{x})$ are the thickness and camber distributions, respectively.

Let $\bar{\phi}(\bar{x},\bar{y})$ be the perturbation velocity potential. The perturbation velocities in the tangential and transverse directions are given by $\bar{u} = \bar{\phi}_{\bar{x}}$ and $\bar{v} = \bar{\phi}_{\bar{y}}$, respectively. The transonic small perturbation equation for $\bar{\phi}$ is

$$[1 - M_\infty^2 - (\gamma + 1)M_\infty^2\,\bar{\phi}_{\bar{x}}\,]\,\bar{\phi}_{\bar{x}\bar{x}} + \bar{\phi}_{\bar{y}\bar{y}} = 0 \tag{2}$$

where M_∞ is the free-stream Mach number and γ is the ratio of specific heats.

Equation (2) is solved subject to the Kutta condition, the body boundary condition,

$$\bar{v}(\bar{x},\pm 0) = \frac{d\bar{Y}_\pm}{d\bar{x}} \tag{3}$$

and the condition that $\bar{u}$ and $\bar{v}$ vanish at infinity.

The following shock jump conditions hold (ref. 10):

$$\left\langle (1 - M_\infty^2)\bar{u} - \frac{M_\infty^2(\gamma + 1)}{2}\bar{u}^2 \right\rangle (d\bar{y})_\Sigma - \langle \bar{v} \rangle (d\bar{x})_\Sigma = 0 \tag{4a}$$

$$\langle \bar{v} \rangle (d\bar{y})_\Sigma + \langle \bar{u} \rangle (d\bar{x})_\Sigma = 0 \tag{4b}$$

where $\langle\ \rangle$ denotes the jump in a quantity across the shock, and the subscript Σ refers to an element on the shock surface.

The transformations, $\beta^2 = 1 - M_\infty^2$, $x = \bar{x}$, $y = \beta\bar{y}$, $\phi(x,y) = [(\gamma + 1)M_\infty^2/\beta^2]\bar{\phi}(\bar{x},\bar{y})$, $u(x,y) = \partial\phi/\partial x$ and $v(x,y) = \partial\phi/\partial y$, reduce (eqs. (2) and (3)) to

$$(1 - \phi_x)\phi_{xx} + \phi_{yy} = 0 \tag{5}$$

$$v(x,\pm 0) = \frac{dY_\pm}{dx} \tag{6}$$

where $Y_\pm(x) = [(\gamma + 1)/\delta K^{3/2}]\bar{Y}_\pm(\bar{x})$ defines the modified airfoil profile and $K = (1 - M_\infty^2)/M_\infty^{4/3}\delta^{2/3}$ is the transonic similarity parameter.

For a normal shock, equations (4a) and (4b) become

$$\left\langle u - \frac{1}{2}u^2 \right\rangle = 0 \tag{7}$$

Let (ξ,ζ) be the running coordinates in the integration; then, for $M_\infty < 1$, application of Green's theorem converts (eqs. (5)-(7)) to the following singular integro-differential equation (refs. 1, 2 and 11):

$$\phi(x,y) = \phi_N(x,y) + \phi_L(x,y) + \iint_S \mathscr{K}(\xi - x,\zeta - y)\phi_\xi^{\,2}(\xi,\zeta)dS \tag{8}$$

where ϕ_N, ϕ_L and $\mathscr{K}$ are defined below.

The contribution to the potential due to nonlifting effects is

$$\phi_N(x,y) = \frac{1}{2\pi}\int_0^1 \Delta\phi_\zeta(\xi)\,\ln[(\xi - x)^2 + y^2]^{1/2}d\xi \tag{9}$$

where

$$\Delta\phi_\zeta(\xi) = \frac{dY_+}{d\xi} - \frac{dY_-}{d\xi} \tag{10}$$

The contribution to the potential due to lifting effects is $\phi_L(x,y)$ and can be written in the following form after an integration by parts (ref. 11):

$$\phi_L(x,y) = \frac{1}{2\pi}\int_0^1\left[\frac{\pi}{2}\operatorname{sgn}(y) - \arctan\left(\frac{\xi - x}{y}\right)\right]\gamma(\xi)d\xi \tag{11}$$

where

$$\gamma(\xi) = u(\xi,+0) - u(\xi,-0) \tag{12}$$

defines the local strength of the vortices distributed along the chord. For a nonlifting airfoil, $\gamma(\xi) = 0$, hence $\phi_L(x,y) = 0$.

The kernel of the integro-differential equation is

$$\mathscr{K}(\xi - x, \zeta - y) = \frac{x - \xi}{4\pi[(\xi - x)^2 + (\zeta - y)^2]} \tag{13}$$

The singular point of the kernel is enclosed in a vanishing rectangular cavity, σ_ε, of aspect ratio λ (fig. 1). The significance of this cavity was reported in a previous article by Ogana and Spreiter (ref. 2).

NONLIFTING EFFECTS

From equations (1) and (10) we deduce that $\Delta\phi_\zeta(\xi) = [2(\gamma + 1)/K^{3/2}]F'(\xi)$. If this relation is substituted in equation (9) and an integration by parts performed, then for an airfoil of unit chord we obtain

$$\phi_N(x,y) = \frac{\gamma + 1}{\pi K^{3/2}} \int_0^1 \frac{x - \xi}{(\xi - x)^2 + y^2} F(\xi)d\xi \tag{14}$$

LIFTING EFFECTS

For lifting airfoils, equation (8) can be solved only after $\gamma(\xi)$ in equation (11) has been determined. To do this we differentiate both sides of equation (8) with respect to y to find

$$v(x,y) = \frac{1}{2\pi} \int_0^1 \frac{y}{(\xi - x)^2 + y^2} \Delta\phi_\zeta(\xi)d\xi + \frac{1}{2\pi} \int_0^1 \frac{\xi - x}{(\xi - x)^2 + y^2} \gamma(\xi)d\xi$$

$$+ \frac{\partial}{\partial y}\left[\iint_S \mathscr{K}(\xi - x, \zeta - y)u^2(\xi,\zeta)dS\right] \tag{15}$$

We now take the limit as $y \to +0$ and $y \to -0$ on both sides of equation (15), add the two results and perform an integral inversion. The procedure, described in appendix A, yields the result

$$\gamma(x) = \mu\alpha \sqrt{\frac{1 - x}{x}} + \frac{\Delta u^2(x,0)}{4}$$

$$+ \sqrt{\frac{1 - x}{x}} \; \frac{2}{\pi} \int_0^1 \frac{G(\xi)}{\xi - x} \sqrt{\frac{\xi}{1 - \xi}} \, d\xi \tag{16}$$

where

$\mu = 2(\gamma + 1)/\delta K^{3/2} = \text{constant}$

$$\Delta u^2(x,y) = u^2(x,y) - u^2(x, -y) \tag{17}$$

$$G(\xi) = \iint_S \chi(x - \xi, y)\Delta u^2(x,y)dx\, dy \tag{18}$$

From equation (A6) we can deduce

$$\chi(x - \xi,y) = \frac{y(\xi - x)}{4\pi[(\xi - x)^2 + y^2]^2} \tag{19}$$

MATRIX EQUATION

Let $P \equiv (x,y)$, $Q \equiv (\xi,\zeta)$ and $\mathscr{K}(Q,P) \equiv \mathscr{K}(\xi - x, \zeta - y)$. Equation (8) can be written

$$\phi(P) = \phi_N(P) + \phi_L(P) + \iint_S \mathscr{K}(Q,P)u^2(Q)dS \tag{20}$$

where

$$u(Q) = \frac{\partial}{\partial \xi}[\phi(Q)] \tag{21}$$

The region of integration, S, is now divided into n rectangular elements, labelled $\Delta_1, \Delta_2, \ldots, \Delta_n$. In each Δ_i there is a mesh point $P_i(x_i,y_i)$, located as shown in figure 1. The mesh points are concentrated near the airfoil and become fewer as the elements grow larger (fig. 2). It is now assumed that the flow quantities are constant within each element. For a mesh point, P_i, equation (20) becomes

$$\phi(P_i) = \phi_N(P_i) + \phi_L(P_i) + \sum_{j=1}^{n} \int_{\Delta_j} \mathscr{K}(Q,P_i)u^2(Q)dS \tag{22}$$

Unless otherwise stated it will be assumed that the subscripts $i, j = 1, 2, \ldots, n$.

Let

$$\phi_i \equiv \phi(P_i),\ \phi_{N_i} \equiv \phi_N(P_i),\ \phi_{L_i} \equiv \phi_L(P_i),\ u_j^2 \equiv u^2(P_j) \tag{23}$$

and define the matrix $[b_{ij}]$ by

$$b_{ij} = \int_{\Delta_j} \mathscr{K}(Q,P_i)dS \tag{24}$$

Then equation (22) becomes

$$\phi_i = \phi_{N_i} + \phi_{L_i} + \sum_{j=1}^{n} b_{ij} u_j^2 \tag{25}$$

When the right-hand side of equation (21) is evaluated numerically, u_j is expressed as a function of the discrete values of the perturbation potential. Equation (25) can then be regarded as a system of nonlinear algebraic equations in $\phi_1, \phi_2, \ldots, \phi_n$. Define the component $g_i(\vec{\phi})$ of the vector $\vec{g}(\vec{\phi})$ by

$$g_i(\vec{\phi}) = \phi_{N_i} + \phi_{L_i} + \sum_{j=1}^{n} b_{ij} u_j^2 \tag{26}$$

In matrix form, equation (25) becomes

$$\vec{\phi} = \vec{g}(\vec{\phi}) \tag{27}$$

where

$$\vec{\phi} = [\phi_1, \phi_2, \ldots, \phi_n]^T \tag{28a}$$

$$\vec{g}(\vec{\phi}) = [g_1(\vec{\phi}), g_2(\vec{\phi}), \ldots, g_n(\vec{\phi})]^T \tag{28b}$$

Equation (14) shows that for a given airfoil profile, ϕ_{N_i} can be evaluated immediately by some suitable numerical integration scheme. Before solutions of equation (27) can be obtained, certain matrices have to be evaluated. Suppose the airfoil is divided into M intervals by the rectangular elements. Using equation (11) we can write ϕ_{L_i} as

$$\phi_{L_i} = \sum_{k=1}^{M} q_{ik} \gamma_k \tag{29}$$

where

$$\gamma_k = \gamma(x_k)$$

$$q_{ik} = \frac{1}{2\pi} \int_{x_k-\delta_k}^{x_k+\delta_k} \left[\frac{\pi}{2} \operatorname{sgn}(y_i) - \arctan\left(\frac{\xi - x_i}{y_i}\right)\right] d\xi \tag{30}$$

The matrix elements, q_{ik}, are evaluated in sec. 1 of appendix B.

To obtain γ_k we let $\Omega(x,y) = \Delta u^2(x,y)$ and $\Omega_k = \Omega(x_k,y_k)$. Equation (16) yields

$$\gamma_k = \mu\alpha\sqrt{\frac{1 - x_k}{x_k}} + \frac{\Omega_k}{4} + \sqrt{\frac{1 - x_k}{x_k}} \sum_{\ell=1}^{M} e_{k\ell} G_\ell \tag{31}$$

where

$$e_{k\ell} = \frac{2}{\pi}\int_{x_\ell-\delta_\ell}^{x_\ell+\delta_\ell} \frac{d\xi}{\xi - x_k}\sqrt{\frac{\xi}{1 - \xi}} \tag{32}$$

Expressions for the matrix elements, $e_{k\ell}$, are derived in sec. 2.1 of appendix B.

In order to evaluate γ_k in equation (31), we require $G_1, G_2, \ldots, G_M$. Using equations (18) and (19) we can obtain

$$G_\ell = \sum_{j=1}^{n} d_{\ell j}\Omega_j \tag{33}$$

where

$$d_{\ell j} = \iint \frac{y(x_\ell - x)}{4\pi[(x_\ell - x)^2 + y^2]^2}\, dx\, dy \tag{34}$$

The matrix elements, $d_{\ell j}$, are determined in sec. 2.2 of appendix B.

The matrix defined by equation (24) is associated with the nonlinear contribution to the potential. It can be written as

$$b_{ij} = \iint_{\Delta_j} \frac{x_i - \xi}{4\pi[(\xi - x_i)^2 + (\zeta - y_i)^2]}\, d\xi\, d\zeta \tag{35}$$

Expressions for the matrix elements, b_{ij}, are derived in sec. 3 of appendix B.

SOLUTION OF THE MATRIX EQUATION

Define $\vec{\phi}_N = [\phi_{N_1}, \phi_{N_2}, \ldots, \phi_{N_n}]^T$. Equation (27) is solved by the Jacobi iteration as follows:

$$\vec{\phi}^{(0)} = \vec{\phi}_N \tag{36a}$$

$$\vec{\phi}^{(m+1)} = \vec{g}[\vec{\phi}^{(m)}], \quad m = 0, 1, 2, \ldots \tag{36b}$$

where the superscript refers to the iteration number.

When solving equation (27) we are confronted with

$$u_j = \left[\frac{\partial\phi}{\partial\xi}\right]_{\xi = x_j \text{ and } \zeta = y_j} \tag{37}$$

Numerical evaluation of this derivative depends on the nature of the local flow as determined by the sign of the coefficient of ϕ_{xx} in equation (5). When $(1 - \phi_x) > 0$, equation (5) is elliptic and describes a local subsonic flow; when $(1 - \phi_x) = 0$, it is parabolic and describes a local sonic flow; and when $(1 - \phi_x) < 0$, it is hyperbolic and describes a local supersonic flow. The difference scheme proposed by Murman and Cole (ref. 10) is designed to solve this type of mixed flow equation. The main feature of the scheme is that, in the tangential direction, central differences are taken in locally subsonic flow regions and backward differences in locally supersonic flow regions. We extend these ideas to the present method.

To simplify the analysis, we assume that the rectangular elements are equal within a given strip parallel to the x-axis (fig. 2). They can differ in size from one strip to another. The mesh points are numbered so that $x_{j+1} > x_j$. Let Δ_x be the width of each element, then $x_{j+1} - x_j = \Delta_x$, for all x_j in the strip.

We define the following two operators at a mesh point P_j:

$$V_E = 1 - \frac{\phi_{j+1} - \phi_{j-1}}{2\Delta x} \tag{38}$$

$$V_H = 1 - \frac{\phi_j - \phi_{j-2}}{2\Delta x} \tag{39}$$

During an iteration, V_E and V_H are computed at each mesh point, P_j. If $V_E > 0$, the flow at P_j is subsonic and equation (37) is evaluated by the central difference formula; i.e.,

$$u_j = \frac{\phi_{j+1} - \phi_{j-1}}{2\Delta x} \tag{40}$$

If $V_E < 0$ and $V_H < 0$, the flow at P_j is supersonic and equation (37) is evaluated by the backward difference formula; i.e.,

$$u_j = \frac{\phi_j - \phi_{j-2}}{2\Delta x} \tag{41}$$

As the flow accelerates through sonic velocity from subsonic to supersonic velocities, a point is reached where $V_E < 0$ and $V_H > 0$. Using the fact that for a locally sonic flow, $1 - \phi_x = 0$, we set

$$u_j = 1 \tag{42}$$

This is analogous to the parabolic point operator (refs. 12 and 13).

As the flow decelerates across the shock from supersonic to subsonic velocities, a point is reached where $V_E > 0$ and $V_H < 0$. Murman (ref. 14) introduced a shock-point operator to be applied at such a point. We use a different approach since it is impractical to extend the shock-point operator concept to the present system. We assume that the mesh point, P_j, where $V_E > 0$ and $V_H < 0$, is located just downstream of the shock. The adjacent mesh point, located upstream of the shock, is P_{j-1}. From equation (7) it can be deduced that

$$u_{j-1} + u_j = 2 \tag{43}$$

If u_{j-1} is given, then u_j can be determined from this equation. The use of u_{j-1} to determine u_j is based on the fact that information propagates downstream in a locally supersonic flow region.

In equations (38) through (41), we could use unevenly spaced grids where appropriate and apply the difference formulas given by Bailey (ref. 15), for instance.

For mesh points adjacent to the far field boundary, equation (37) is evaluated using a method which Ames (ref. 16) described for derivatives near a boundary. If the far field boundary is infinitely far from the airfoil, the potential on it could be held fixed through all iterations. The computational region does not, in practice, extend very far. Consequently, it is best to update the potential on the far field boundary after a few iterations.

Before solving equation (27), it is important to give careful consideration to the number of mesh points required. Figure 2 shows the elements growing larger the farther they are from the airfoil. This type of partitioning enables computation to be performed in a large region of integration while using a small number of mesh points. It also ensures that the significant contribution from mesh points near the airfoil is not dispersed in unusually large elements. For a given distribution of the elements, the computational region can be extended by increasing the aspect ratios of the elements.

RESULTS AND DISCUSSION

Figures 3 and 4 show the coefficient of pressure plots for a nonlifting parabolic-arc airfoil of thickness ratio $\delta = 0.06$ at free-stream Mach numbers 0.825 and 0.87, respectively. Figure 5 shows the coefficient of pressure plots for a NACA 0012 at $\alpha = 2°$ and $M_\infty = 0.63$. The results for the present method are compared with those of a finite difference scheme by Ballhaus, Jameson and Albert (ref. 17) in figure 5. The finite difference method uses a 67x41 mesh point network; convergence is achieved in 40 to 100 iterations, depending on the free-stream Mach number.

In comparison, the present method uses about 200 mesh points located in rectangular elements whose aspect ratios range from 2 to 8. Iteration proceeds until the largest difference between successive iterates is smaller than some specified tolerance; i.e.,

$$\max_i \left| \phi_i^{(m+1)} - \phi_i^{(m)} \right| < t \tag{44}$$

where t is the tolerance.

The rate of convergence for the present method, applied to the parabolic-arc airfoil, is shown in the following tabulation for two tolerance values.

M_∞	Tolerance	Iterations
0.825	10^{-3}	4
	10^{-4}	7
0.870	10^{-3}	12
	10^{-4}	20

The results presented are obtained when the potential on the far field boundary is updated after each iteration. If the potential on the boundary is held fixed, there is a noticeable effect on values near the boundary, but that effect diminishes in the interior.

Near the leading edge of a lifting airfoil, the accuracy of the method could be improved by applying a modified boundary condition described by Nixon (refs. 7 and 18).

CONCLUDING REMARKS

The present study indicates that the integro-differential equation method can provide rapid and reliable solutions for transonic flow problems. Contrary to what happens in the integral equation schemes, the shock conditions are enforced in a simple and straightforward manner. Although a relatively small number of mesh points is used, the results agree well with finite difference computations.

Extension to three-dimensional lifting flows can be made provided it is possible to determine the equivalent of the integral inversion that yields an expression for the vortex strength. There should be no fundamental problems in applying the present scheme to nonlifting three-dimensional flows.

APPENDIX A

VORTEX STRENGTH

The vortex strength, $\gamma(x)$, is determined by solving the following linear integral equation

$$v(x,y) = \frac{1}{2\pi}\int_0^1 \frac{y}{(\xi - x)^2 + y^2} \Delta\phi_\zeta(\xi)d\xi + \frac{1}{2\pi}\int_0^1 \frac{\xi - x}{(\xi - x)^2 + y^2} \gamma(\xi)d\xi$$
$$+ \frac{\partial}{\partial y}\left[\iint_S \mathscr{K}(\xi - x,\ \zeta - y)u^2(\xi,\zeta)dS\right] \tag{15}$$

where $\Delta\phi_\zeta(\xi)$ is given by equation (10) and $\mathscr{K}(\xi - x, \zeta - y)$ by equation (13).

We now take the limit as $y \to \pm 0$ on both sides of equation (15) and add the two results.

Karamcheti (ref. 19) shows that

$$\lim_{y \to \pm 0} \frac{1}{2\pi}\int_0^1 \frac{y}{(\xi - x)^2 + y^2} \Delta\phi_\zeta(\xi)d\xi = \pm\frac{1}{2}\Delta\phi_\zeta(x) \tag{A1}$$

Mangler (ref. 20) shows that

$$\lim_{y \to \pm 0} \frac{1}{2\pi}\int_0^1 \frac{\xi - x}{(\xi - x)^2 + y^2} \gamma(\xi)d\xi = \frac{1}{2\pi}\oint_0^1 \frac{\gamma(\xi)}{\xi - x} d\xi \tag{A2}$$

where the right-hand side is a Cauchy integral.

Nixon and Hancock (ref. 5) have evaluated the last term in equation (15) as $y \to \pm 0$. From equations (1) and (6) we deduce

$$v(x,+0) + v(x,-0) = \mu[\tau H'(x) - \alpha] \tag{A3}$$

where the constant $\mu = 2(\gamma + 1)/\delta K^{3/2}$.

Using equation (A3) together with the results obtained when $y \to \pm 0$ on the right-hand side of equation (15) we conclude

$$\frac{1}{2}\mu\left[\tau H'(x) - \alpha\right] = -\frac{1}{2\pi}\oint_0^1 \frac{\gamma(\xi)}{x - \xi}\,d\xi + \frac{1}{2\pi}\oint_0^1 \frac{\Delta u^2(\xi,0)}{4(x - \xi)}\,d\xi$$

$$+ \iint_S \chi(\xi - x,\zeta)\,\Delta u^2(\xi,\zeta)\,dS \tag{A4}$$

where

$$\Delta u^2(\xi,\zeta) = u^2(\xi,\zeta) - u^2(\xi,-\zeta) \tag{A5}$$

$$\chi(\xi - x,\zeta) = \frac{\zeta(x - \xi)}{4\pi\left[(\xi - x)^2 + \zeta^2\right]^2} \tag{A6}$$

When the terms are suitably arranged, equation (A4) can be inverted to give an explicit expression for $\gamma(x)$. We define

$$\Delta W(\xi) = \gamma(\xi) - \frac{\Delta u^2(\xi, 0)}{4} \tag{A7}$$

$$G(x) = \iint_S \chi(\xi - x,\zeta)\,\Delta u^2(\xi,\zeta)\,d\xi\,d\zeta \tag{A8}$$

$$W_o(x) = \frac{1}{2}\mu\left[\tau H'(x) - \alpha\right] - G(x) \tag{A9}$$

Substitution of equations (A7) - (A9) into equ tion (A4) yields

$$W_o(x) = -\frac{1}{2\pi}\oint_0^1 \frac{\Delta W(\xi)}{x - \xi}\,d\xi \tag{A10}$$

Ashley and Landahl (ref. 21) show that equation (A10) can be inverted to give

$$\Delta W(x) = \frac{2}{\pi}\sqrt{\frac{1 - x}{x}}\int_0^1 \frac{W_o(\xi)}{x - \xi}\sqrt{\frac{\xi}{1 - \xi}}\,d\xi \tag{A11}$$

We consider an airfoil without camber and use the following result from Ashley and Landahl (ref. 21):

$$\frac{1}{\pi}\int_0^1 \frac{d\xi}{x - \xi}\sqrt{\frac{\xi}{1 - \xi}} = -1 \tag{A12}$$

Substituting for $\Delta W(x)$ and $W_o(\xi)$, we obtain the expression

$$\gamma(x) = \mu\alpha\sqrt{\frac{1 - x}{x}} + \frac{\Delta u^2(x,0)}{4} + \sqrt{\frac{1 - x}{x}}\,\frac{2}{\pi}\int_0^1 \frac{G(\xi)}{\xi - x}\sqrt{\frac{\xi}{1 - \xi}}\,d\xi \tag{A13}$$

APPENDIX B

MATRIX ELEMENTS

In this appendix we derive expressions for some matrix elements which are required in the numerical solution of the integro-differential equation.

1. Matrix Associated with the Contribution of Lift to the Potential

The matrix associated with the contribution of lift to the potential at a mesh point $P_i(x_i, y_i)$ is given by

$$q_{ik} = \frac{1}{2\pi} \int_{x_k-\delta_k}^{x_k+\delta_k} \left[\frac{\pi}{2} \operatorname{sgn}(y_i) - \operatorname{arc\,tan}\left(\frac{\xi - x_i}{y_i} \right) \right] d\xi \tag{30}$$

where $i = 1,2, \ldots, n$, $k = 1,2, \ldots, M$, and $y_i \neq 0$.

Equation (30) can be evaluated at once to give

$$\begin{aligned} q_{ik} = \frac{1}{2\pi} \Bigg\{ & \pi\delta_k \operatorname{sgn}(y_i) - (x_k - x_i + \delta_k) \operatorname{arc\,tan}\left(\frac{x_k - x_i + \delta_k}{y_i} \right) \\ & + (x_k - x_i - \delta_k) \operatorname{arc\,tan}\left(\frac{x_k - x_i - \delta_k}{y_i} \right) \\ & + \frac{y_i}{2} \ln\left[\frac{y_i^2 + (x_k - x_i + \delta_k)^2}{y_i^2 + (x_k - x_i - \delta_k)^2} \right] \Bigg\} \end{aligned} \tag{B1}$$

for $y_i = \pm 0$.

We have to consider separately three values of x_i, namely, $x_i < x_k$, $x_i = x_k$ and $x_i > x_k$. Integration of equation (30) yields the result

$$q_{ik} = \left\{ \begin{array}{ll} 0, & x_i < x_k \\ \frac{1}{2}\delta_k \operatorname{sgn}(y_i), & x_i = x_k \\ \delta_k \operatorname{sgn}(y_i), & x_i > x_k \end{array} \right\} \tag{B2}$$

2. Matrices Associated with the Vortex Strength

There are two matrices associated with the vortex strength; one arises from a double integral before an inversion is performed and the other arises from a line integral after the inversion.

2.1 Matrix from the Line Integral

The matrix element is given by

$$e_{k\ell} = \frac{2}{\pi}\int_{x_\ell-\delta_\ell}^{x_\ell+\delta_\ell} \frac{d\xi}{\xi - x_k}\sqrt{\frac{\xi}{1-\xi}} \quad , \quad \ell,k = 1,2,\ldots,M \tag{32}$$

Let $t = \xi - x_k$, $b = x_k$, $a = 1 - x_k$, $t_2 = x_\ell - x_k + \delta_\ell$, $t_1 = x_\ell - x_k - \delta_\ell$. Equation (32) is transformed to

$$e_{k\ell} = \frac{2}{\pi}\int_{t_1}^{t_2} \frac{dt}{t}\sqrt{\frac{b+t}{a-t}} \tag{B3}$$

The substitution $r^2 = (b + t)/(a - t)$ converts the integral to one which can be evaluated easily to give

$$e_{k\ell} = \frac{4}{\pi}\left[T(t_2) - T(t_1)\right] \tag{B4}$$

where

$$T(t) = \arctan\sqrt{\frac{b+t}{a-t}} + \frac{1}{2}\sqrt{\frac{b}{a}}\,\ln\left|\frac{\sqrt{a(b+t)} - \sqrt{b(a-t)}}{\sqrt{a(b+t)} + \sqrt{b(a-t)}}\right| \tag{B5}$$

2.2 Matrix from the Double Integral

The matrix element is given by

$$d_{\ell j} = \iint_{\Delta_j} \frac{y(x_\ell - x)}{4\pi[(x_\ell - x)^2 + y^2]^2}\,dx\,dy \tag{34}$$

where $\ell = 1,2,\ldots,M$ and $j = 1,2,\ldots,n$

Coordinates of P_ℓ and P_j not Identical

If the coordinates of $P_\ell(x_\ell,y_\ell)$ and $P_j(x_j,y_j)$ are not identical, then equation (34) involves a non-singular integral which can be evaluated at once. Substitution of the limits of integration yields

$$d_{\ell j} = \int_{y_j-q_j}^{y_j+r_j} \int_{x_j-\delta_j}^{x_j+\delta_j} \frac{y(x_\ell - x)}{4\pi\left[(x_\ell - x)^2 + y^2\right]^2} \, dx \, dy \tag{B6}$$

Hence

$$d_{\ell j} = -(1/16\pi) \ln (N/D) \tag{B7}$$

where

$$N = \left[(y_j + r_j)^2 + (x_j - x_\ell - \delta_j)^2\right]\left[(y_j - q_j)^2 + (x_j - x_\ell + \delta_j)^2\right]$$

$$D = \left[(y_j - q_j)^2 + (x_j - x_\ell - \delta_j)^2\right]\left[(y_j + r_j)^2 + (x_j - x_\ell + \delta_j)^2\right]$$

The quantities δ_j, r_j and q_j are defined as shown in figure 1. Let $2h_j$ be the height of Δ_j, then

$$2h_j = r_j + q_j \tag{B8}$$

The quantities r_j and q_j are chosen as follows:

$$r_j = q_j = h_j \tag{B9}$$

if P_j is at the center of Δ_j; or

$$r_j = 2h_j \text{ and } q_j = 0 \tag{B10}$$

if P_j is at the bottom edge of Δ_j; or

$$r_j = 0 \text{ and } q_j = 2h_j \tag{B11}$$

if P_j is at the top edge of Δ_j.

Coordinates of P_ℓ and P_j Identical

The coordinates of $P_\ell(x_\ell,y_\ell)$ and $P_j(x_j,y_j)$ can be identical even if $\ell \neq j$. This occurs if P_ℓ and P_j are both on the airfoil, have the same x-coordinate, but are situated on opposite sides of the airfoil. If the coordinates of P_ℓ and P_j are identical, equation (34) contains a single integral. Following the method by Ogana (refs. 6 and 9), the integral is evaluated after enclosing the singularity in a vanishing retangular cavity, σ_ε (fig. 1); i.e.,

$$d_{\ell j} = \lim_{\varepsilon \to 0} \left[\iint_{\Delta_j - \sigma_\varepsilon} \frac{y(x_\ell - x)}{4\pi \left[(x_\ell - x)^2 + y^2 \right]^2} \right] dx\, dy \tag{B12}$$

Substitution of the limits of integration and subsequent evaluation yields

$$d_{\ell j} = 0 \tag{B13}$$

3. Matrix Associated with the Nonlinear Contribution to the Potential

The matrix associated with the contribution of the nonlinear effects to the potential at a mesh point $P_i(x_i, y_i)$ is

$$b_{ij} = \iint_{\Delta_j} \frac{x_i - \xi}{4\pi \left[(\xi - x_i)^2 + (\zeta - y_i)^2 \right]} d\xi\, d\zeta \tag{35}$$

Diagonal Elements

If Δ_j contains P_i, then $P_i \equiv P_j$ and diagonal elements are obtained. The integral in equation (35) becomes singular at $P_i(x_i, y_i)$. Following the method by Ogana (refs. 6 and 9), integration is performed after enclosing the singularity in a vanishing rectangular cavity, σ_ε (fig. 1). Equation (35) is consequently defined as follows:

$$b_{ii} = \lim_{\varepsilon \to 0} \left[\iint_{\Delta_i - \sigma_\varepsilon} \frac{x_i - \xi}{4\pi \left[(\xi - x_i)^2 + (\zeta - y_i)^2 \right]} d\xi\, d\zeta \right] \tag{B14}$$

The appropriate integration steps yield

$$b_{ii} = 0 \tag{B15}$$

Off-diagonal Elements

If P_i does not belong in Δ_j, off-diagonal elements are obtained by evaluating equation (35) written in the form

$$b_{ij} = \int_{y_j - q_j}^{y_i + r_j} \int_{x_j - \delta_j}^{x_j + \delta_j} \frac{x_i - \xi}{4\pi\left[(\xi - x_i)^2 + (\zeta - y_i)^2\right]} \, d\xi \, d\zeta \tag{B16}$$

Since there are no singularities, this integral can be evaluated at once to give

$$b_{ij} = -(1/4\pi)\left[A_1 + A_2 + A_3 + A_4\right], \qquad i \neq j \tag{B17}$$

where

$$A_1 = \frac{1}{2}(y_j - y_i + r_j)\ \ell n\left[\frac{(x_j - x_i + \delta_j)^2 + (y_j - y_i + r_j)^2}{(x_j - x_i - \delta_j)^2 + (y_j - y_i + r_j)^2}\right]$$

$$A_2 = \frac{1}{2}(y_j - y_i - q_j)\ \ell n\left[\frac{(x_j - x_i - \delta_j)^2 + (y_j - y_i - q_j)^2}{(x_j - x_i + \delta_j)^2 + (y_j - y_i - q_j)^2}\right]$$

$$A_3 = (x_j - x_i + \delta_j)\left[\arctan\left(\frac{y_j - y_i + r_j}{x_j - x_i + \delta_j}\right) - \arctan\left(\frac{y_j - y_i - q_j}{x_j - x_i + \delta_j}\right)\right]$$

$$A_4 = (x_j - x_i - \delta_j)\left[\arctan\left(\frac{y_j - y_i - q_j}{x_j - x_i - \delta_j}\right) - \arctan\left(\frac{y_j - y_i + r_j}{x_j - x_i - \delta_j}\right)\right]$$

where r_j and q_j are chosen according to equations (B8) - (B11).

REFERENCES

1. Heaslet, M. A.; and Spreiter, J. R.: Three-Dimensional Transonic Flow Theory Applied to Slender Wings and Bodies. NACA Rep. 1318, 1957.

2. Ogana, W.; and Spreiter, J. R.: Derivation of an Integral Equation for Transonic Flows. AIAA Journal, vol. 15, no. 2, 1977, pp. 281-283.

3. Spreiter, J. R.; and Alksne, A. Y.: Theoretical Predictions of Pressure Distributions on Nonlifting Airfoils at High Subsonic Speeds. NACA Rep. 1217, 1955.

4. Norstrud, H.: High-Speed Flow Past Wings. NASA CR-2246, 1973.

5. Nixon, D; and Hancock, G. J.: High Subsonic Flow Past a Steady Two-Dimensional Aerofoil. ARC CP1280, 1974.

6. Ogana, W.: Computation of Steady Two-Dimensional Transonic Flows by an Integral Equation Method. Ph.D. Thesis, Stanford University, Calif., 1976.

7. Nixon, D.: Calculation of Transonic Flows Using an Extended Integral Equation Method. AIAA Paper No. 75-876, 1975.

8. Morino, L.; and Kuo, C. C.: Subsonic Potential Aerodynamics for Complex Configurations: A General Theory. AIAA Journal, vol. 12, no. 2, 1974, pp. 191-197.

9. Ogana, W.: Numerical Solution for Subcritical Flows by a Transonic Integral Equation Method. AIAA Journal, vol. 15, no. 3, 1977, pp. 444-446.

10. Murman, E. M.; and Cole, J. D.: Calculation of Plane Steady Transonic Flows. AIAA Journal, vol. 9, no. 1, 1971, pp. 114-121.

11. Klunker, E. B.: Contribution to Methods for Calculating the Flow About Thin Lifting Wings at Transonic Speeds - Analytical Expression for the Far Field. NASA TN D-6530, 1971.

12. Murman, E. M.; and Krupp, J. A.: Solution of the Transonic Potential Equation Using a Mixed Difference System. Lecture Notes in Physics, vol. 8, Springer-Verlag, 1971, pp. 199-206.

13. Bailey, F. R.: On the Computation of Two- and Three-Dimensional Steady Transonic Flows by Relaxation Methods. Lecture Notes in Physics, vol. 41, Springer-Verlag, 1975, pp. 1-77.

14. Murman, E. M.: Analysis of Embedded Shock Waves Calculated by Relaxation Methods. AIAA Journal, vol. 12, no. 5, 1974, pp. 626-633.

15. Bailey, F. R.: Numerical Calculation of Transonic Flow About Slender Bodies of Revolution. NASA TN D-6582, 1971.

16. Ames, W. F.: Numerical Methods for Partial Differential Equations. Barnes and Noble, 1971.

17. Ballhaus, W. F.; Jameson, A.; and Albert, J.: Implicit Approximate-Factorization Schemes for the Efficient Solution of Steady Transonic Flow Problems. NASA TM X-73,202, 1977.

18. Nixon, D.: An Alternative Treatment of Boundary Conditions for the Flow over Thick Wings. Aeronaut. Quart. Vol. XXVIII, 1977, pp. 90-96.

19. Karamcheti, K.: Principles of Ideal-Fluid Aerodynamics. John Wiley & Sons, Inc., 1966.

20. Mangler, K. W.: Improper Integrals in Theoretical Aerodynamics. A.R.C., R&M 2424, 1951.

21. Ashley, H.; and Landahl, M.: Aerodynamics of Wings and Bodies. Addison Wesley, 1965.

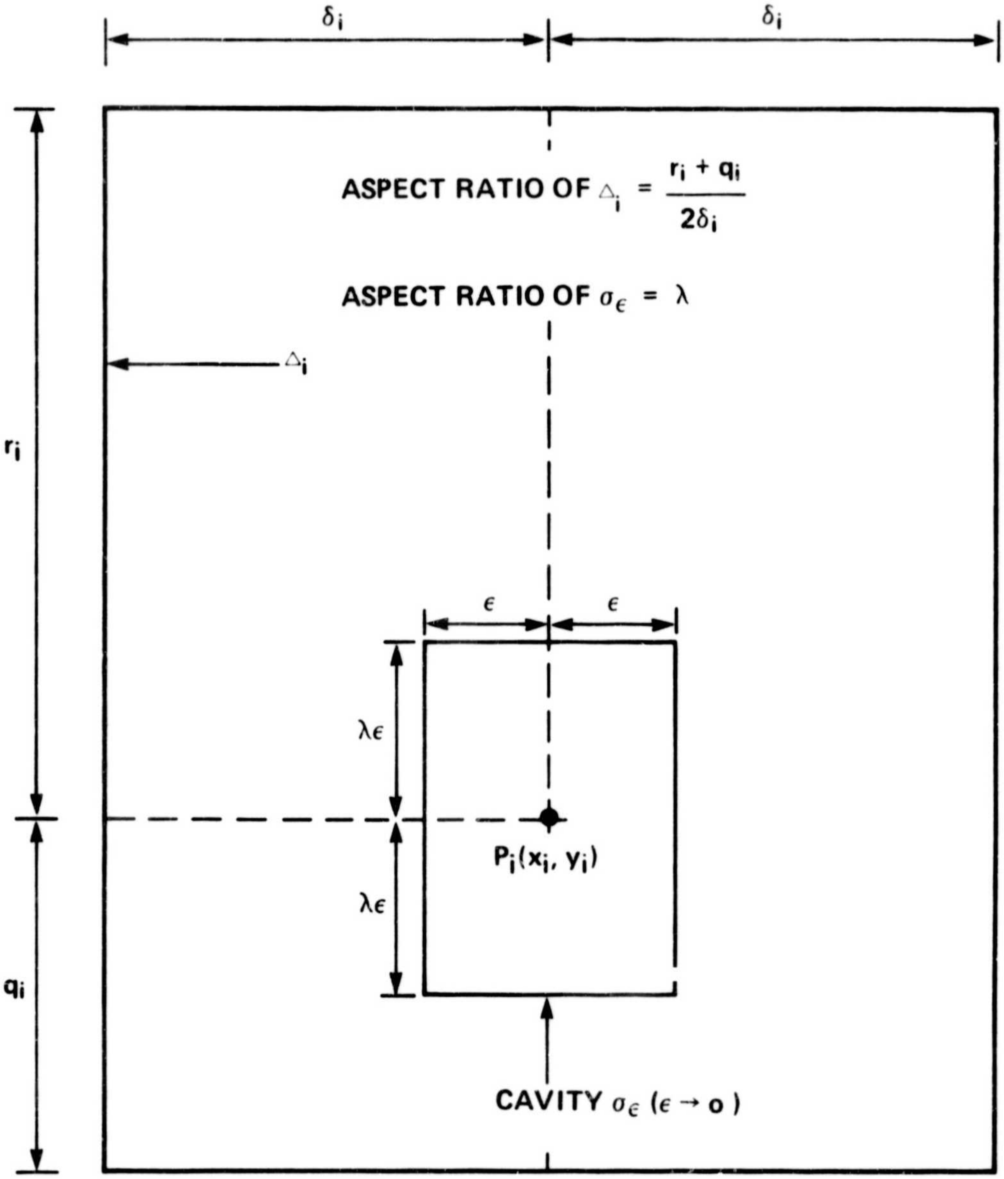

Figure 1.- Location of mesh point, P_i, in the rectangular element, Δ_i.

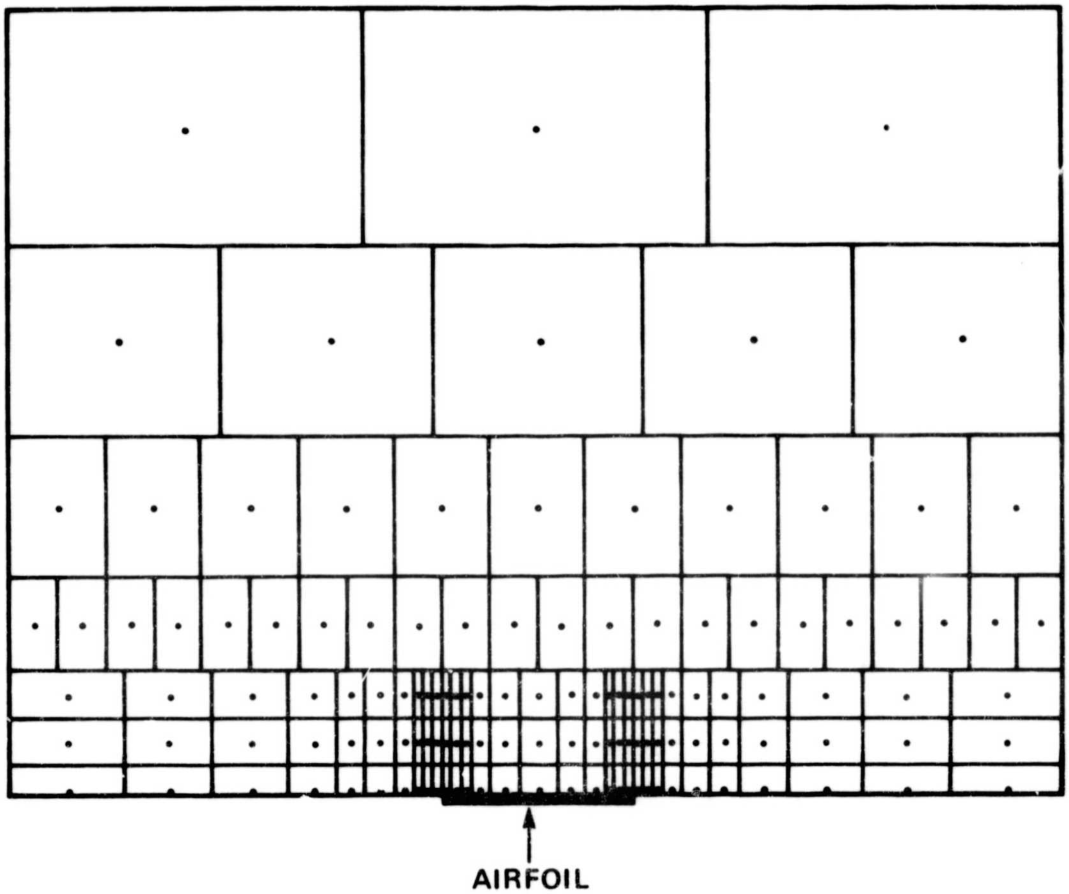

Figure 2.- Distribution of mesh points and rectangular elements in the upper half plane.

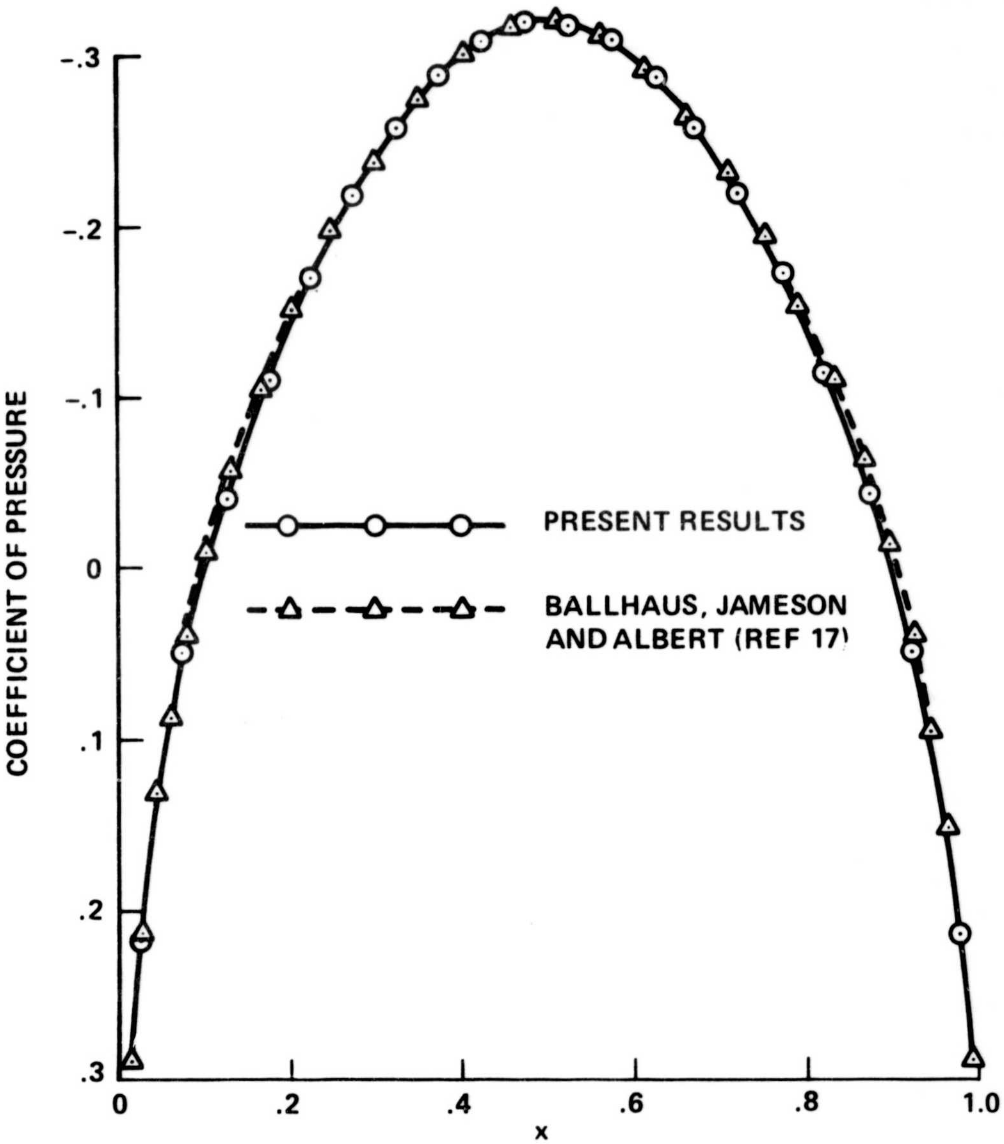

Figure 3.- Coefficient of pressure for a parabolic-arc airfoil of thickness ratio 0.06, at M_∞ = 0.825.

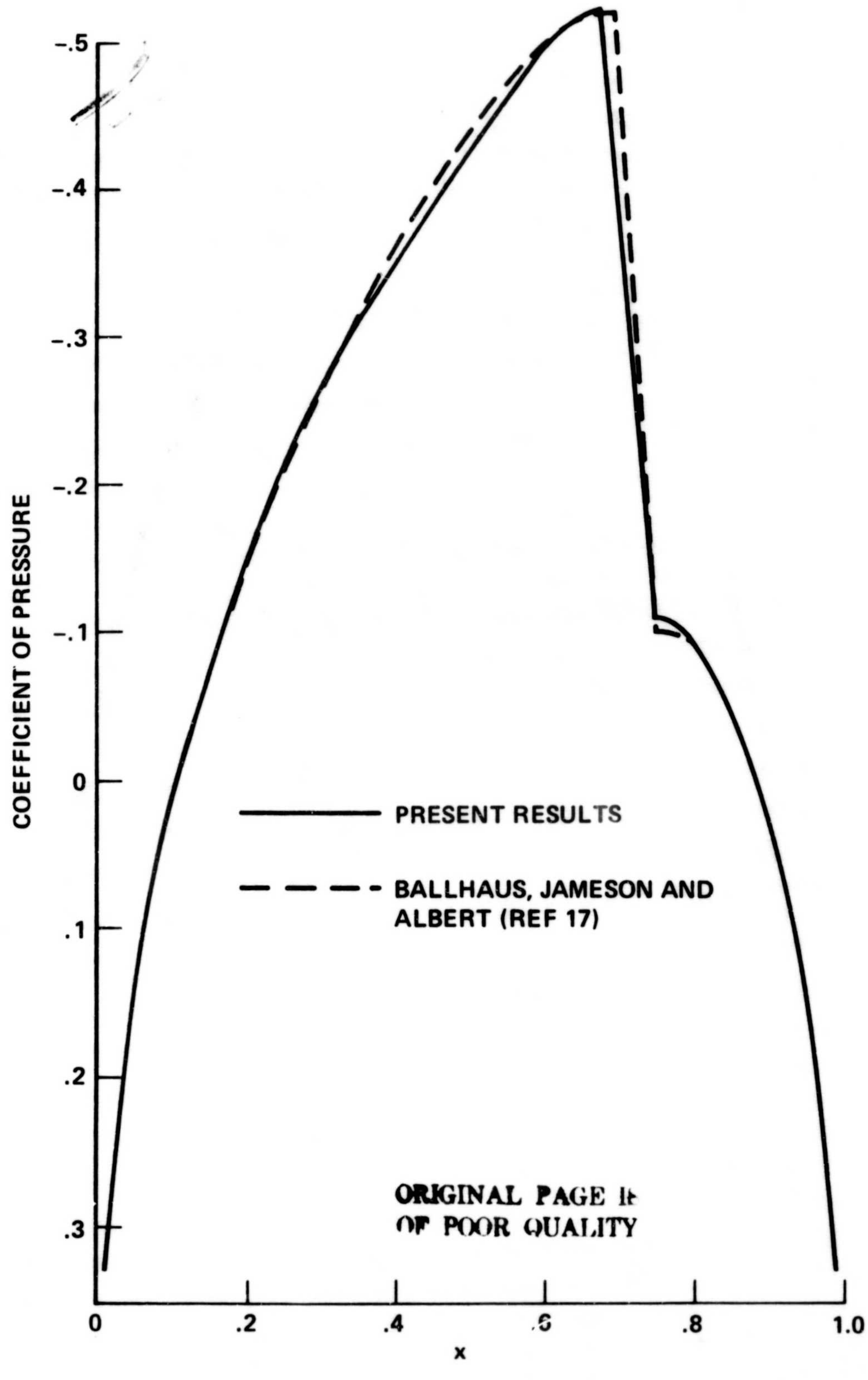

Figure 4.- Coefficient of pressure for a parabolic-arc airfoil of thickness ratio 0.06, at M_∞ = 0.87.

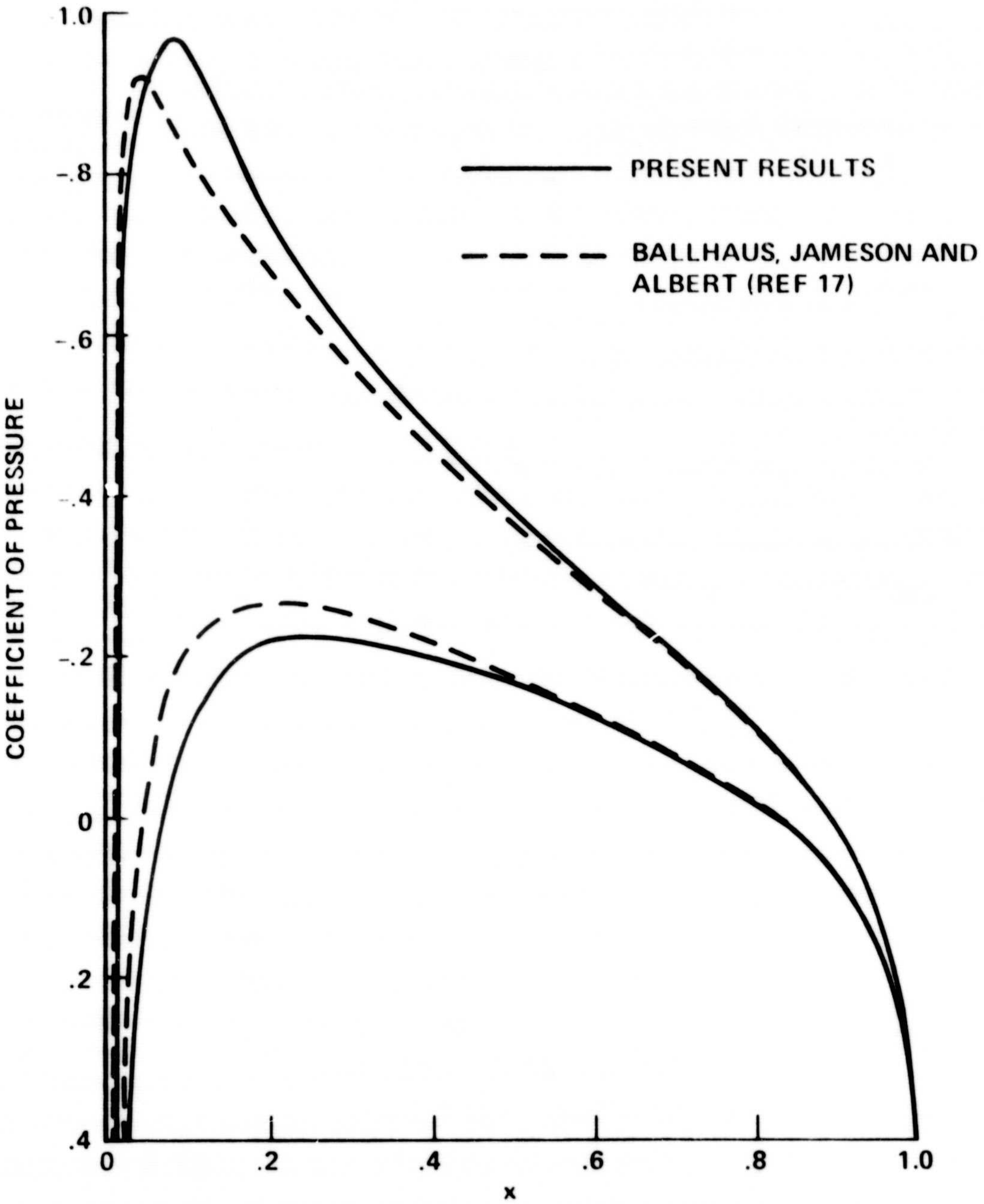

Figure 5.- Coefficient of pressure for NACA 0012 at $M_\infty = 0.63$ and $\alpha = 2°$.

1. Report No.	2. Government Accession No.	3. Recipient's Catalog No
NASA TM-78490		

4. Title and Subtitle	5. Report Date
SOLUTION OF TRANSONIC FLOWS BY AN INTEGRO-DIFFERENTIAL EQUATION METHOD	
	6. Performing Organization Code
7. Author(s)	8. Performing Organization Report No.
Wandera Ogana*	A-7434
	10. Work Unit No.
9. Performing Organization Name and Address	505-06-11
NASA Ames Research Center Moffett Field, Calif. 94035	11. Contract or Grant No.
	13. Type of Report and Period Covered
12. Sponsoring Agency Name and Address	Technical Memorandum
National Aeronautics and Space Administration Washington, D.C. 20546	14. Sponsoring Agency Code

15. Supplementary Notes

*National Research Council Research Associate (1976-1977). Presently a Lecturer at University of Nairobi, Department of Mathematics, P.O. Box 30197, Nairobi, Kenya.

16. Abstract

Solutions of steady transonic flow past a two-dimensional airfoil are obtained from a singular integro-differential equation which involves a tangential derivative of the perturbation velocity potential. Subcritical flows are solved by taking central differences everywhere. For supercritical flows with shocks, central differences are taken in subsonic flow regions and backward differences in supersonic flow regions. The method is applied to a nonlifting parabolic-arc airfoil and to a lifting NACA 0012 airfoil. Results compare favorably with those of finite-difference schemes.

17. Key Words (Suggested by Author(s))	18. Distribution Statement
Transonic flow Integro-differential equation	Unlimited STAR Category — 34

19. Security Classif. (of this report)	20. Security Classif. (of this page)	21. No. of Pages	22. Price*
Unclassified	Unclassified	30	$4.00

*For sale by the National Technical Information Service, Springfield, Virginia 22161

ORIGINAL PAGE IS OF POOR QUALITY